Pergamon

SCIENCE DIRECT®

Tetrahedron 59 (2003) 3821–3831

TETRAHEDRON

Dendrimers with tetrabenzoporphyrin cores: near infrared phosphors for in vivo oxygen imaging

Ivo B. Rietveld, Evelyn Kim and Sergei A. Vinogradov*

Department of Biochemistry and Biophysics, University of Pennsylvania, Philadelphia, PA 19104, USA

Received 28 November 2002; revised 22 January 2003; accepted 4 February 2003

Abstract—Pd complexes of tetrabenzoporphyrins (PdTBPs) are strong near infra-red phosphors, suitable for tissue oxygen imaging by phosphorescence quenching. For in vivo use, PdTBP phosphors have to be water-soluble and protected from interactions with biomacromolecules in the blood. An approach to the construction of biologically compatible PdTBP-phosphors based on dendritic encapsulation is proposed. A series of polyglutamic PdTBP-dendrimers was synthesized and their optical and quenching properties were studied. While retaining the excellent optical characteristics ($\lambda_{max\ Q}$=630 nm, ϕ_{phos}=12%) of basic PdTBPs and in addition being highly water soluble, PdTBP-dendrimers still exhibit excessively high oxygen quenching constants (2000–3000 $mmHg^{-1}\ s^{-1}$) and form complexes with lipophilic proteins, such as serum albumin. Modification of the dendrimer periphery with polyethyleneglycol chains somewhat reduces the quenching constants but does not prevent binding of the phosphors to albumin.

1. Introduction

The growing interest in dendrimers over the past years has been due to their unique molecular design, which offers numerous possibilities in catalysis, construction of nano-scale electro-optical devices, drug delivery and other applications.[1] Although very attractive from the standpoint of basic research, the mass monodispersity and monodispersity of physical properties of dendrimers, comes at the high cost of multistage synthesis, which often diminishes the practicality of dendritic materials. Indeed, in only a few applications have the unique structural characteristics of dendrimers been able to justify the tedious synthetic and purification procedures, which often leads to a preference for imperfect, but much less expensive hyperbranched polymers.

In such applications, monodispersity must prevail over cost considerations, and this requirement is often met in bio-medicine. For example, in medical imaging it is desirable that physical properties of imaging agents are distributed within a narrow range; otherwise, heterogeneity of image tracers can result in reduced resolution of the imaging modality itself. It is also important that an exogenous dye or a contrast agent has a well-defined, reproducible and predictable biodistribution, which is most reliably achieved through the use of monodisperse materials. In this context, it is not surprising that MR imaging using dendritic contrast agents was one of the first proposed uses of dendrimers.[2] In this application, the possibility to attach multiple functionalities, i.e. paramagnetic Gd^{3+} complexes, on the dendrimer periphery has been exploited, resulting in contrast agents with a significantly increased circulation lifetime and with a well defined bio-distribution.

Another opportunity that dendrimers offer for construction of bio-medical imaging agents is encapsulation of a functional moiety,[3] leading to its isolation from components of in vivo systems and, as a result, elimination of the potential for toxicity. The construction of imaging agents, specifically of phosphorescent probes for in vivo oxygen measurements, employing this approach has been the focus of our research in the past few years.

Quantification of dissolved molecular oxygen (O_2) using luminescence quenching is a well-known methodology. A large number of oxygen sensors based on polymer supported luminescent dyes has been described in the past, and some of these have become available commercially.[4] In many biological applications, however, it is advantageous to directly fuse the medium of interest with soluble oxygen tracer, rather than to insert optodes, which inflict mechanical damage and decreases measurement accuracy. During the past decade, the former approach[5] has been used to measure and image oxygen in both in vitro and in vivo experimental systems.[6] For clinical applications the phosphorescence quenching technique has potential in the diagnosis and evaluation of complications from diabetes, peripheral vascular diseases, cerebrovascular and cardiovascular events, and eye pathology (such as diabetic

Keywords: porphyrin; laterally extended porphyrin; dendrimer; dendritic encapsulation; oxygen; non-invasive imaging; phosphorescence; luminescence; quenching.

* Corresponding author. Tel.: +1-215-898-6382; fax: +1-215-573-3787; e-mail: vinograd@mail.med.upenn.edu

0040–4020/03/$ - see front matter
doi:10.1016/S0040-4020(03)00432-0

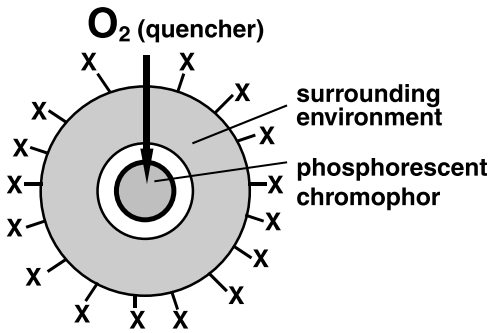

Figure 1. Scheme of phosphorescent indicator for in vivo applications.

retinopathy and macular degeneration), as well as the detection of tumors and the design of their therapeutic treatment.

The effectiveness of phosphorescence quenching by oxygen is determined by the frequency of collision between the triplet state molecules and O_2. In systems where O_2 is the primary quencher (as in most biological systems) phosphorescence lifetime is related to oxygen concentration (pressure) by the Stern–Volmer equation:

$$I_0/I = \tau_0/\tau = 1 + K_q\tau_0[O_2], \quad (1)$$

where I_o and τ_o are the phosphorescence intensity and the lifetime in the absence of oxygen, I and τ are the intensity and the lifetime at a concentration $[O_2]$, and K_q is the rate constant of the reaction between the triplet state phosphor and O_2. The value of K_q depends on the diffusion constants of phosphor and O_2, temperature, and phosphor microenvironment. The Stern–Volmer relationship holds as long as the concentration of the quencher molecules is much higher than that of the triplet state phosphor. This is generally true for all common applications, i.e. when the concentration of oxygen is above 10^{-8} M and the concentration of the excited phosphor is less than 10^{-14} M.

Practical oxygen measurement consists of the following steps: the phosphor is delivered to the medium of interest (i.e. injected in the blood in vivo), the object is illuminated with light of appropriate wavelength, the emitted phosphorescence is collected and its time course analyzed to give the oxygen concentration. When the measurement is performed in vivo, it is desirable that the phosphor be removed from the medium (i.e. blood) upon completion of the measurement. Each of the listed steps imposes requirements on the choice of the dye, which is the only 'invasive' component in the entire scheme.

An optical oxygen sensor for biological imaging in general is a combination of two components: phosphorescent chromophor and its surrounding environment (Fig. 1).

For in vivo applications the properties of the chromophor must include strong absorption bands in the near 'infra-red window' of tissue (between 620 and 900 nm), to minimize the interference of natural chromophors (heme proteins etc.), room temperature phosphorescence with high quantum yield (>5%) and sufficiently long lifetime. The lifetimes of several tens of μs are generally acceptable, although longer lifetimes (100–1000 μs) are preferred for higher oxygen sensitivity.

The surrounding environment assures biological compatibility of the entire probe, i.e. water solubility and protection from interactions with active components of the blood. The overall size of the construct should be adequate to permit its clearance from the body via kidney dialysis (less than 15 kDa). Another important function of the surrounding shell is to control oxygen access to the chromophor, i.e. the value of the constant K_q (Eq. (1)). Excessively high K_q's, typical of unprotected phosphors, decrease the dynamic range of the method, since both the phosphorescence lifetime and the intensity become too low already at intermediate O_2 levels. To achieve the best accuracy in measurement the K_q values must be in the range of 100–400 $mmHg^{-1}\,s^{-1}$, which in water translates into about $0.6–2.4\times10^8\ M^{-1}\,s^{-1}$ on the molar scale.[7]

One way to build oxygen sensor molecules of the kind shown in Figure 1 is to encapsulate Pd (or Pt) porphyrins, which are widely used as basic phosphors,[5,6] inside dendrimers. Dendrimers surrounding luminescent chromophors have been shown to increase diffusion barriers for oxygen[8] and other quenchers in solution.[9] Considerable literature exists on dendritic encapsulation of porphyrins. Porphyrin-dendrimers have been studied with the purpose of building mimics of natural heme containing enzymes,[10] channeling the transfer of electrons via dendritic architecture,[9a,11] creating selective oxidation catalysts[12] and light harvesting systems.[13] In our own work, we have demonstrated that dendrimers control the access of O_2 to Pd-porphyrin cores, and that varying the dendrimer size enables tuning of phosphorescence oxygen quenching properties.[14] In the case of more hydrophobic dendrimers, folding of the lipophilic dendritic matrix in water diminishes the mobility of the protecting shell and enhances oxygen diffusion barriers.[15] At the same time, multiple peripheral functionalities serve as anchor points for linking hydrophilic modifiers (PEGs, polyalcohols, etc.), which minimize interactions with proteins and other macromolecules in vivo, making phosphorescent sensors specific only to oxygen.

All previous work on dendritic encapsulation of porphyrins has been done using regular tetraarylporphyrins (Ar_4P). Many of these porphyrins are readily available via Alder–Longo[16] or Lindsey type[17] condensations, and their electrooptical properties are well studied. Pd and $PtAr_4Ps$ have excellent phosphorescent characteristics[18] and in principle are well suited for oxygen measurements. However, visible absorption Q-bands of these compounds are located between 500 and 550 nm, where many tissue chromophors also strongly absorb light. As a result, when used for tissue applications, Pd and $PtAr_4P$-phosphors permit oxygen measurements only in very thin superficial layers of tissue. Carrying excitation at wavelengths above 600 nm would considerably increase the depth of tissue sampling. A few near infra-red porphyrinic dyes with characteristics appropriate for tissue oxygen sensing have been reported in the literature.[19,20] Among them, tetrabenzoporphyrins (TBPs) and especially tetraaryltetrabenzoporphyrins (Ar_4TBPs) appeared to be most well suited for in

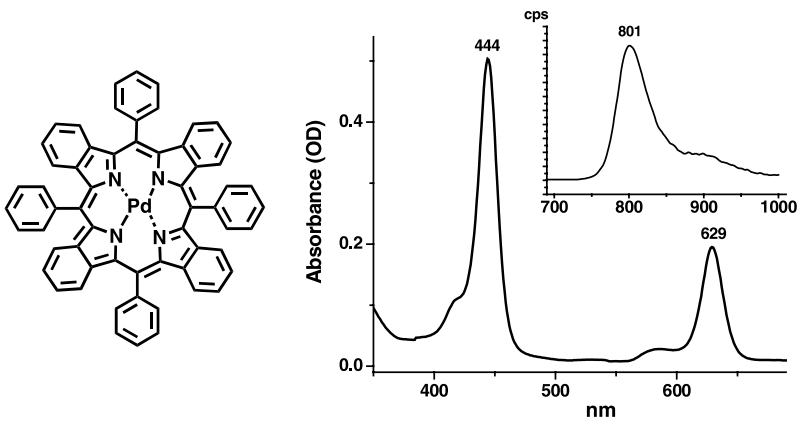

Figure 2. Structure, absorption and emission properties of Pd *meso*-tetraphenyltetrabenzoporphyrin ($PdPh_4TBP$). Phosphorescence quantum yield of $PdPh_4TBP$ in deoxygenated pyridine, measured using red-sensitive detection system (see Section 3 for details), is 16.6% and the lifetime is 195 μs.

vivo applications.[5c] $PdAr_4TBPs$ strongly absorb light above 630 nm ($\varepsilon \approx 50{,}000$) and emit phosphorescence ($\lambda_{max} \approx 700$ nm) with lifetimes of about 300 μs and quantum yields of about 10–12% in deoxygenated solutions at room temperature.[20a] Primitive soluble derivatives of Pd *meso*-tetraphenyltetrabenzoporphyrin ($PdPh_4TBP$, Fig. 2) proved to be good basic O_2 sensors in aqueous solutions.[5c,20b]

In this paper we report first dendritic tetrabenzoporphyrins, analogues of earlier reported polyglutamic Pd porphyrin-dendrimers.[14] Tetrabenzoporphyrin-dendrimers build a bridge between porphyrin-dendrimers and phthalocyanine-dendrimers,[21] forming a group of new near infra-red dyes for in vivo applications.

2. Results and discussion

2.1. Synthesis of functionalized tetraaryltetrabenzoporphyrin (Ar_4TBP) cores

In order to be used as cores for dendrimers, *meso*-tetraaryltetrabenzoporphyrins (Ar_4TBPs) must bear peripheral functional groups, to which dendrons can be attached. The synthesis of functionalized tetrabenzoporphyrins, however, presents a challenging problem. Until very recently all synthetic methods leading to Ar_4TBPs were based on high temperature condensation between phthalimide and phenylacetic acids, or similar donors of benzo- and phenyl-groups.[22,23] The harsh conditions of this process (fusion at 350–400°C) allowed for only a few inert substituents to be introduced into the macrocycle.

Recently new strategies were proposed for TBP synthesis.[24] All these methods employ Barton–Zard chemistry for the synthesis of various porphyrinogenic pyrroles, further used to produce TBP precursors, i.e. porphyrins requiring final aromatization. Although far superior in their versatility and yield (total 10–20% of target Ar_4TBPs), all new methods involve multi-step syntheses of precursor compounds. It was, therefore, of interest to check if the template condensation approach, which requires very inexpensive starting materials and entails a one-step synthetic scheme, could at least in some cases be of comparable practicality for generating Pd complexes of Ar_4TBPs, suitable for initiation of dendrimer growth. In this work we used this approach to produce Pd *meso*-tetra-4-carboxyphenyltetrabenzoporphyrin (**4**).

The synthesis used in this work is shown in Scheme 1.

The key step is the fusion of Zn *para*-bromophenylacetate

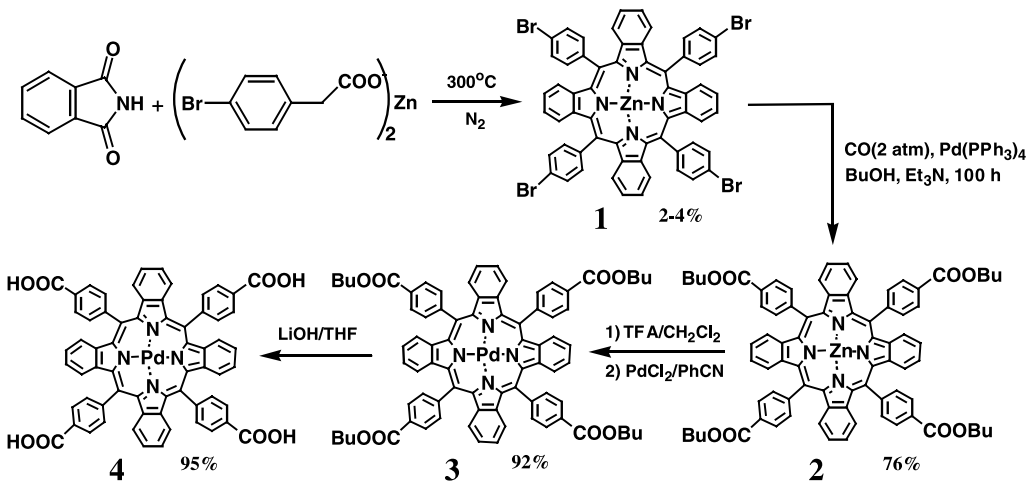

Scheme 1.

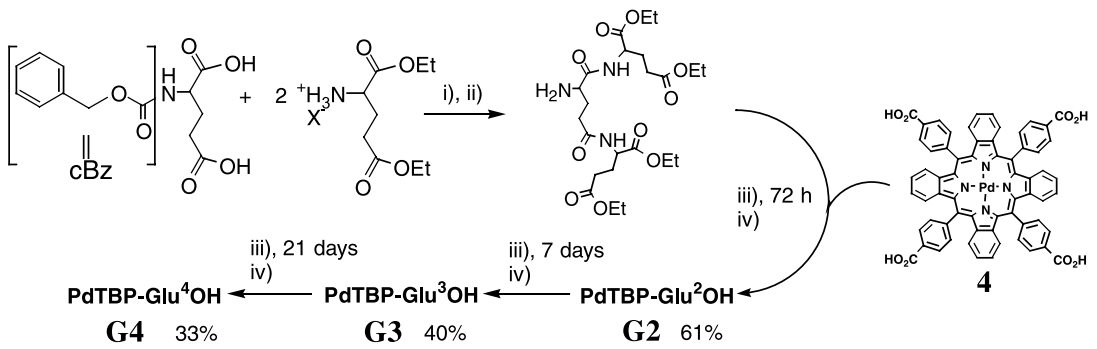

Scheme 2. (i) DCC, pyridine, THF, rt, 48 h; (ii) H_2, Pd/C, THF/MeOH, rt, 72 h, 65%; (iii) DCC/BtOH (hydroxybenzotriazole), pyridine, DMF, rt; (iv) LiOH/THF/MeOH, rt; (iv) DCC, pyridine, DMF, rt.

with phthalimide. This reaction results in a mixture of products, from which target Zn-tetrabromotetrabenzoporphyrin (**1**) can be isolated only in a very low yield (1–2%). We found that using pre-synthesized Zn salt of bromophenylacetic acid is more advantageous than the traditionally employed $ZnCl_2$ or Zn-benzoate.[25] Purification after the template condensation is the most time consuming step in the whole scheme. At least three chromatographies are required to produce **1** of sufficient purity. The steps following purification, however, are simple and occur with high yields. The brominated porphyrin is first converted into its tetra-butoxycarbonyl derivative **2** by Pd(0) catalyzed carbonylation.[26] The choice of butyl alcohol is dictated primarily by the higher solubility of the starting material in this solvent. The latest results, however, reveal that methoxycarbonylation can be carried equally well in the MeOH/THF mixture. In both cases, product **2** appears contaminated with small (5–10%), but reproducibly detectable amounts of the corresponding Pd complex **3**. It's formation is probably due to partial oxidative decomposition of the Pd-catalyst ($Pd(0)(PPh_3)_4$) and the displacement of Zn with Pd(II) in the TBP core, favored by extremely high thermodynamic stability of Pd tetrabenzoporphyrins. The alkoxycarbonylated porphyrin **2** is then fully converted into **3** by displacing Zn and inserting Pd into the resulting porphyrin free-base. The latter is hydrolyzed under basic conditions giving target compound **4**.

Since one of our goals was to maximize the yield of **4** with minimal effort expended in the purification of the intermediate products, we also investigated the possibility of synthesis without intermediate isolation of Zn-complexes and free-base tetrabenzoporphyrins. Following the condensation, the resulting solid was extracted with THF in a Soxleht extractor and the resulting mixture was purified only once on neutral alumina, to separate most of the non-porphyrinic contaminants. The thus obtained mixture of ZnTBPs was introduced directly into carbonylation using roughly 20–50 mol% of the catalyst. Following the reaction, Zn was replaced with Pd using the same sequence of reaction as in Scheme 1, and only after that the product was purified chromatographically. The chromatography was performed twice: once with CH_2Cl_2, or chloroform, and once with toluene. The last chromatography is very time consuming, but allows for the complete separation of **3** (MW 1318) from its main contaminant tri-*meso*-aryl-substituted $Pd(4\text{-}BuOOCC_6H_4)_3TBP$ (MW 1218). Subsequent hydrolysis quantitatively yields **4**. Overall, the sequence affords porphyrin **4** in 1–2% yield, and employs in total three chromatographies. As mentioned before, the obtained yield is considerably lower than that achieved by all new methods,[24] but the ease of the procedure makes this approach worth consideration.

2.2. Synthesis of PdTBP-dendrimers

The synthesis of polyglutamic dendrimers with similar Pd porphyrin cores has been described in detail previously.[14] In the present work we synthesized compounds of the general formula PdTBP-Glu^NOR, where PdTBP is the core tetrabenzoporphyrin **4**, Glu^N is the dendritic glutamic layer of the generation *N* (*N*=1–4), and R is the terminal group. Diethyl ester of L-glutamic acid was used as a building block for dendritic polyglutamates. Some of the dendrimers were modified with terminal polyethyleneglycol monomethylethers of average molecular weight 350, designated as PEG350, according to the methods described earlier.[10c,27] Therefore, terminal groups R in the dendrimers were H, Et and PEG350. Pegylation has been previously utilized in other bio-medical applications with the purpose of constructing neutral micelle-like biocompatible dendrimers.[28] For convenience, the carboxyl-terminated compounds, PdTBP-Glu^NOH, will be designated throughout the text as **GN** (*N*=1–4), while the ester-terminated dendrimers PdTBP-Glu^NOR will be termed as **GN-R**, where *N*=1–4 and R=Et or PEG350.

The generation 1 dendrimer (**G1**) was produced by coupling four glutamic acid diesters to the core **4** in 96% yield. The generation 2 triglutamic dendron was synthesized convergently[15,29] and linked to **4** using standard DCC chemistry, giving the generation 2 dendrimer (**G2**). The generation 3 and 4 dendrimers (**G3** and **G4**) were synthesized in divergent sequence, starting with **G2**, similar to the earlier reported scheme.[14] Synthesis of dendrimers **G2**–**G4** is shown in Scheme 2.

All the synthesized compounds were characterized by ^1H, ^{13}C NMR and, in the case of the ethyl esters **GN-Et** (*N*=1–4) and carboxyl-terminated dendrimers **G1** and **G2** by MALDI-TOF mass spectroscopy. The esters **G1-Et** (MW 1834) and **G2-Et** (MW 3092) exhibited single peaks in MALDI spectra, while **G3-Et** (MW 5608) showed an additional satellite peak at MW 5294. This is believed to be due to fragmentation, not to an underderivatized product. This peak is 314 mass units below the molecular ion (M^+),

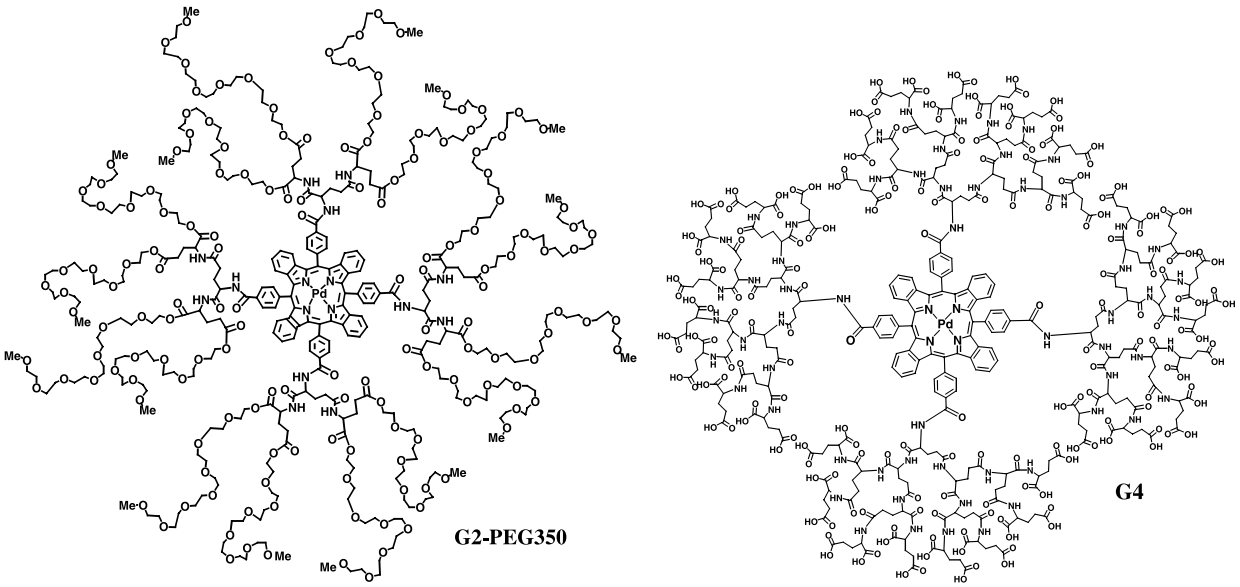

Figure 3. Selected PdTBP-dendrimers synthesized in this work.

while the satellites with missing glutamic fragments would have masses decreasing in multiples of 185. Similarly, the **G4-Et** dendrimer (MW 10,630) showed a multiplet of peaks decaying from the M^+ in the steps of 314. The MALDI spectra of PEG350 adducts, **G*N*-PEG350** (N=1–2), showed broad peaks with no fine structure. The examples of the synthesized molecules are shown in Figure 3.

2.3. Properties of PdTBP-dendrimers

All the synthesized dendrimer-esters are well soluble in THF, dimethylformamide (DMF) and pyridine. PEG350-terminated compounds are also soluble in water. The photophysical characteristics of ester terminated dendrimers in organic solvents almost exactly match those of the parent tetrabenzoporphyrin **4**, indicating that dendritic branches attached to the *para*-positions of *meso*-phenyl rings in the porphyrin have almost no influence on the core.

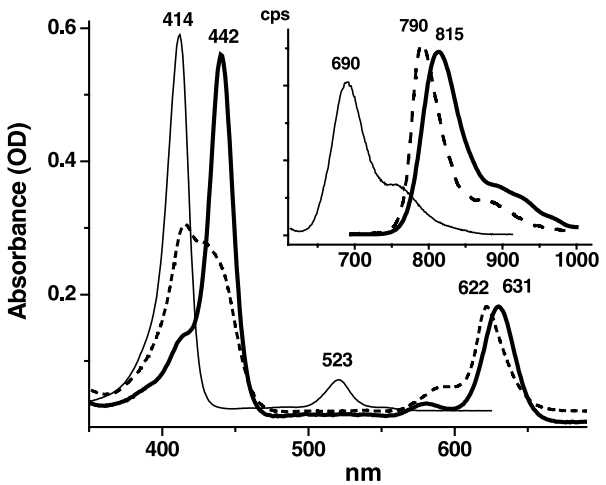

Figure 4. Absorption (main graph) and emission (inset) spectra of dendrimer **G3** (▬), tetrabenzoporphyrin **4** (– –) and PdTCPP (—) in aqueous solutions. The spectra of dendrimers **G1**, **G2** and **G4** almost exactly match those of **G3**.

Carboxylic acid PdTBP-terminated dendrimers, **G1**–**G4**, are soluble in water at basic and neutral pH, and their solubility increases significantly with an increase in the dendrimer generation and thus in the number of peripheral carboxylates. All PdTBP-dendrimers exhibit strong near infra-red Q-bands and infra-red phosphorescence at room temperature. Examples of absorption and emission spectra of dendrimers are shown in Figure 4 together with the spectrum of the parent tetrabenzoporphyrin **4** and PdTCPP for comparison. The properties of water-soluble PdTBP-dendrimers are summarized in Table 1.

The absorption spectrum of **4** reveals significant aggregation, practically unaffected by the increase in pH up to 12. Both Soret and Q-bands are blue shifted and broadened, which is probably due to the formation of H-type face-to-face porphyrin aggregates,[30] and the phosphorescence maximum is also blue-shifted by about 25 nm. Judging from their absorption and emission spectra, the PdTBP-dendrimers **G1**–**G3** exhibit only traces of aggregation in water. The aggregates completely disappear upon addition of Tween 80 (a non-ionic detergent). Dendrimer **G4** is non-aggregated at pH 8.5, and the same is true for the PEG350-derivatives. At pH below 1.0, however, dendrimer **G4** also begins showing some traces of aggregation, although its precipitation by acidification is not possible. In general, compared to the analogous dendrimers with PdTCPP as a core, PdTBP-dendrimers are much more soluble in organic solvents but substantially less soluble in aqueous media. Even compound **G3** could be precipitated from aqueous solutions upon addition of acid. Along with their higher hydrophobicity, PdTBP-dendrimers have a greater tendency to form aggregates than do PdTCPP-dendrimers, in this respect more resembling phthalocyanine-dendrimers.[21d] This fact, as well as the ease with which parent tetrabenzoporphyrin **4** forms π-stacked aggregates in spite of its high non-planarity[31] suggests

Table 1. Properties of water soluble polyglutamic PdTBP-dendrimers of generation N (N=0–4)

No.	Compound	MW	λ_{max} (Soret, Q) (nm)	λ_{max} (emiss) (nm)	ϕ (%)[a]	K_q (H_2O) (mm Hg^{-1} s^{-1})	τ_0 (H_2O) (μs)
0	**4**	1094	415, 622[b]	790	12.74±0.22	1507±5	394
1	**G1**	1610	443, 632	815	12.71±0.26	3196±17	191
	G1-PEG350	4266	433, 624[b]	805	–	1074±4	295
2	**G2**	2642	443, 632	815	13.01+0.35	3426±11	199
	G2 (BSA)[c]	–	443, 633	817	–	182±2	344
	G2-PEG350	7954	443, 632	818	–	1094±2	323
	G2-PEG350 (BSA)[c]	–	442, 631	818	–	211±32[d]	
3	**G3**	4706	442, 631	815	10.97±0.75	3789±14	164
4	**G4**	8834	442, 631	815	9.17±0.34	2902±7	137

Measurements were made in phosphate buffer at pH 8.5.
[a] Phosphorescence quantum yields (ϕ) were measured using excitation at Q-band. The solutions were deoxygeanted using glucose/glucose oxidase/catalase enzymatic system.[5]
[b] Soret and Q-bands are broadened and shifted due to aggregation.
[c] Solution contains 1.5% of Bovine Serum Albumin (BSA).
[d] Exhibits non-linear Stern–Volmer plot.

quite high hydrophobicity of the core tetrabenzoporphyrin itself. Face-to-face aggregation of PdTBP-dendrimers is favored because it minimizes contacts of hydrophobic porphyrin planes with water. At the same time, back-folding of dendritic polyglutamic branches, attached to the *para*-positions of the porphyrin phenyl rings, is obviously not sufficient in preventing porphyrin-water contacts.

All synthesized compounds (**G0**–**G4**) exhibit strong oxygen dependent phosphorescence with λ_{max} ranging from 790 to 818 nm. The first unexpected result (see Table 1) is that in spite of strong aggregation, the phosphorescence quantum yield of parent porphyrin **4** in water (12.7%) is not decreased compared to much less aggregated PdTBP-dendrimers. Typically, aggregation of emitting species leads to an increase in the probability of non-radiative deactivation of excited states, presumably via the self-quenching. This is most certainly true for triplet state emitters, such as Pd and Pt-porphyrins,[32] and has been demonstrated for phthalocyanines, including phthalocyanine-dendrimers.[21d] In the present case, however, no obvious self quenching has been detected, and, in fact, the quantum yield of **4** is one of the highest in the series.

Another interesting feature observed is that the oxygen quenching constant (K_q) of completely unprotected **4** (1507 $mmHg^{-1}$ s^{-1}) is significantly lower than K_qs of PdTBP-dendrimers. At the same time, the lifetime at zero-oxygen (τ_0) is significantly longer (394 vs 130–200 μs). It should be mentioned, that despite the highly efficient deoxygenating system employed in our studies (glucose/glucose oxidase/catalase),[33] we could frequently detect a correlation between the values of quenching constants and the measured lifetimes τ_0, which almost certainly can be explained by the presence of residual O_2. Therefore, increased τ_0 of **4** can be explained by its lower quenching constant. However, it is the decrease in oxygen quenching (K_q) itself that is rather unexpected. One possible explanation of this phenomenon would be that the capping of one porphyrin surface by another porphyrin in a face-to-face aggregate results in roughly half-reduced oxygen access, compared to a molecule which is open on both sides. Indeed, the observed quenching constant of aggregated **4** is about two times lower than K_qs of the dendrimers. Such an interpretation would be valid, of course, only if the quenching of phosphorescence in aggregates is limited by O_2 diffusion. This, however, is likely to be the case, since Stern–Volmer plots of **4** exhibit good linearity.

By analogy with porphyrin-dendrimers[34] and phthalocyanine-dendrimers,[21d] positioning of dendritic substituents in the *para*-positions of *meso*-phenyl rings in tetrabenzoporphyrins would be expected to have just a minor, if any, effect on the core-porphyrin. Indeed, in the series of polyglutamic Pd porphyrin-dendrimers[14] the maximal protection achieved in the generation 4 dendrimer resulted in only a 4-fold decrease in K_q value compared to the generation 1 dendrimer.[35] Nevertheless, a steady decline in K_q values has been detected throughout the whole series. In the presented here PdTBP-series, however, the situation is quite different. Only **G4** shows a measurable drop in K_q (2902 $mmHg^{-1}$ s^{-1}), while from **G1** to **G3** the quenching constants actually rise in values (from 3196 to 3789 $mmHg^{-1}$ s^{-1}). The apparent lifetimes, τ_0, vary slightly, but in general they are not much different from that of $PdPh_4TBP$ (195 μs) (Fig. 2). The increase in K_q values in the sub-series **G1** –**G3** can be attributed again only to intermolecular aggregation. Although affecting oxygen diffusion rates, the aggregation again, as in the case of the parent porphyrin **4**, has almost no effect on the emission quantum yields and on the spectra of dendrimers, suggesting that distances between PdTBP-cores in the aggregates are quite large. Both aggregation and protection by dendritic wedges is minimal in the case of dendrimer **G3**. In the smaller dendrimers, **G1** and **G2**, protection is low, and the decrease in apparent K_q values is entirely due to the presence of non-self quenching intermolecular aggregates. In contrast, 64 ionized peripheral carboxylates (pH 8.5) in **G4** prohibit molecules from forming intermolecular contacts, and at the same time, larger dendritic branches begin creating a measurable diffusion barrier for O_2.

PdTBP-dendrimers bind tightly to bovine serum album (BSA), which produces a substantial effect on their quenching properties. Albumin is present in the blood serum in vivo in about 4% concentration, and, since it possesses multiple lipophilic binding sites, it can alter the luminescent properties of porphyrins.[36] Table 1 shows that the addition of 1.5% BSA to the solution of **G2** results in an almost 20-fold decrease of its oxygen quenching constant, suggesting that a tight complex forms between the protein and the PdTBP-dendrimer. The values of the quenching

constant (182 $mmHg^{-1}$ s^{-1}) and the lifetime τ_0 (344 μs) remain unchanged upon further increase in the BSA concentration. More detailed studies have shown that **G2** can be used as a phosphor for in vivo measurements,[37] since it does not require pre-binding to bovine albumin and forms complexes with endogenous albumin after being injected in the blood.

Modification of PdTBP-dendrimer termini with hydrophilic neutrally charged monomethoxypolyethyleneglycol chains (PEG350) produced a significant decrease in quenching constants of both **G1** and **G2** compounds. PEG-esterification had a similar effect on polyglutamic and some other Pd porphyrin-dendrimers,[15] suggesting that bulky PEG residues in water create an additional steric barrier for oxygen diffusion. The ultimate goal of pegylation, however, has been to reduce the effect of albumin on the quenching properties of PdTBP-dendrimers, since an ideal oxygen probe must have luminescent characteristics independent of the measurement medium. In previous studies we have demonstrated that modification of some Pd-porphyrin dendrimers with PEGs makes it possible to solve this problem.[15] In the present case, however, the effect of albumin on PEG-modified dendrimer **G2-PEG350** was still very large. The quenching constant of the latter was about 5 times different in the presence of BSA compared to simple water solution (see Table 1). In addition, significant non-linearity of Stern–Volmer plot revealed multiple aggregates between BSA and **G2-PEG350**. This is typical for phosphors which only partially bind to BSA.

In conclusion, PdTBP-dendrimers appear to be good water-soluble, near infra-red oxygen sensors for in vivo applications. It is clear, however, that in order to reach the required degree of core protection and to diminish core-to-core aggregation, dendrons must be attached to other than *para*-positions in the porphyrin *meso*-rings. This will become possible when tetrabenzoporphyrins with appropriately positioned anchor functional groups are available. Synthesis of such cores is currently in progress.

3. Experimental

3.1. Equipment and methods

^1H and ^{13}C spectra were recorded on Varian Unity-500 and Brucker AMX-300 spectrometers, TMS was used as the internal standard. Optical spectra were recorded on a Perkin–Elmer Lambda 35 UV–VIS spectrophotometer. Steady state fluorescence and phosphorescence measurements were performed on a Fluorolog Spex 2 fluorometer, equipped with near infra-red sensitive Hamamatsu R2658P photomultiplier. MALDI-TOF analysis was performed in Wistar Institute of the University of Pennsylvania on a Voyager 6030 (Applied Biosystems Inc.) system, using α-cyano-4-hydroxycinnamic acid as a matrix.

Phosphorescence lifetime measurements and [Lifetime vs Oxygen]-titrations were performed using a system constructed 'in house'. Two main components of the system are a frequency domain phosphorometer (Oxygen Enterprises, Ltd.)[38] and a special Clark-type oxygen electrode.[39] The special design of the electrode causes its zero-current to be in the order of a few *p*A, while the noise at this level is only about 4%, permitting highly accurate O_2 measurements even at very low O_2 concentration (<0.05 mmHg). At least three data sets were independently acquired for each compound, providing required experimental statistics.

Phosphorescence quantum yields were determined using aqueous solutions deoxygenated by glucose (20 mM)/glucose oxidase/catalase enzymatic system, as previously reported.[5] Pyridine solutions were deoxygenated by bubbling of Ar (Grade 6, BOC Gases, Inc.) until no further changes in phosphorescence lifetimes were detected, after which the cuvettes were sealed. The absorbances of the samples at Q-band maxima, used for excitation, were kept below 0.05 OD. The quantum yields were obtained by computing the integrals of the corrected emission spectra and referenced to the fluorescence quantum yield of H_2TPP (ϕ_{fluor}=11%)[40] or ZnTPP in deoxygenated benzene (ϕ_{fluor}=3.3%).[41] The spectra were normalized by the optical density of the samples at the excitation wavelength, relative photon intensity of the source and quantum efficiency of the detector throughout the emission range.

3.2. Synthesis

Column chromatography was carried out on alumina (Aldrich, activated, neutral, Brockmann I, standard grade, ~150 mesh, 58 Å) and on silica gel (Aldrich, Merck, grade 9385, 230–400 mesh, 60 Å). GPC was carried out on Biorad Biobeads S-X1 (mobile phase: THF) and Sephadex G-50 (mobile phase: H_2O). $Pd(0)(PPh_3)_4$ for carbonylation was purchased from Pressure Chemical Company (Pittsburgh, PA), all other reagents and solvents were purchased from Aldrich, Inc. and Fisher Scientific, Inc. Diglutamic dendron (Scheme 2) was synthesized according to the published methods.[15,29] $PdPh_4TBP$ for reference quantum yield and lifetime measurements was synthesized as described previously.[20,23] Synthesis of all PdTBP-dendrimers was carried out under dry N_2 or Ar. Solutions of light sensitive compounds were shielded from ambient light. In the reported below UV–VIS data for the porphyrins, the intensities (shown in parenthesis) are given relative to the strongest absorption in the spectrum, i.e. the Soret band, whose intensity was set to 1.0.

3.2.1. $Zn(4\text{-}BrC_6H_4CH_2COO)_2$. 4-Bromophenylacetic acid (94.6 g, 0.44 mol) and NaOH (17.9 g, 0.45 mol) were stirred in 1.5 L of water in a 2 L beaker, until the solution became clear. A solution of $ZnCl_2$ (30.3 g, 0.22 mol) in 75 mL of water was added to the mixture at once with continuous stirring. The addition was followed by the formation of a bulky white precipitate. To complete the crystallization the beaker was kept at 4°C overnight, after which the white precipitate was filtered, washed on the filter with three 200 mL portions of cold water and dried in vacuum. Yield: 93.3 g (86%).

3.2.2. Zn *meso*-$(4\text{-}BrC_6H_4)_4TBP$ (1) and Zn *meso*-$(4\text{-}BuOOCC_6H_4)_4TBP$ (2). $(4\text{-}BrC_6H_4CH_2COO)_2Zn$ (46.74 g, 94.8 mmol) and phthalimide (27.7 g, 0.19 mol) were mixed together and placed in a jar, fitted with a gas inlet and an outlet. The jar was immersed in a sand bath and heated to

380°C under a continuous flow of Ar. When the temperature was about 150°C, a large amount of water separated and was carried out by the gas. The mixture was kept under 380–390°C for 1 h. and then cooled down. The resulting black shiny solid was transferred into a large Soxleht extractor and extracted with hot pyridine for 24 h. The resulting deep green solution was reduced in volume down to approximately 150 mL and CH_2Cl_2 (200 mL) was added. The mixture was filtered through the paper filter (Whatman, Grade 5) on a Buchner funnel, leaving a fine brown precipitate. The resulting solution was passed through a column with alumina, eluting with CH_2Cl_2/pyridine (4:1). The green fractions were collected, while all black material (impurities) was adsorbed on the column. The solvent was removed on a rotary evaporator, leaving 6.15 g of dark green amorphous solid, consisting mainly of **1**. Pure **1** could be isolated as a dark green solid after additional chromatography of a sample mixture using silica gel and eluting with CH_2Cl_2/THF (10:1), followed by removal of the solvent in vacuum. δ_H (DMF-d_7): 8.21–8.11 (16H, $AA'BB'_{Ar}$), 7.29–7.13 (16H, $AA'BB'_{benzo}$); MALDI, *m/z*: found 1195, calcd 1193 for $C_{60}H_{32}Br_4N_4Zn$; UV–VIS, λ_{max} nm (DMF): 469 (1.0), 614 (0.06), 658 (0.14).

Butoxycarbonylation of brominated Zn tetrabenzoporphyrin(s) was carried out according to the earlier published method.[26] All solid material, collected at the previous stage, was placed in a 250 mL vessel (Ace Glass, Inc.) together with $Pd(PPh_3)_4$ (1.0 g, 0.87 mmol), PPh_3 (1.5 g, 5.7 mmol), 150 mL of BuOH and 15 mL of Et_3N. The vessel was immersed in an oil bath, and the mixture was kept under continuos stirring and CO flow until the temperature was brought up to 90°C. The vial was sealed and the pressure was raised up to 2.5 atm. The mixture was left to react under continuous stirring for 7 days. The heating was stopped and the vessel was depressurized. The resulting dark green solution was filtered, the solvents were removed by rotary evaporation and the remaining green solid was vacuum dried overnight. The material was redissolved in 50 mL of CH_2Cl_2 and chromatographed on silica gel, eluent CH_2Cl_2/THF=10:1. The main deep green fraction was collected, the solvent was evaporated and the resulting green material was dried in vacuum. Chromatography of a small amount (~2% of the total weight) of this material (silica gel, CH_2Cl_2/THF=20:1) allowed the isolation of **2** as a major green band with R_f ~0.5. The rest of the solid was used in the following synthesis without additional purification. δ_H ($CDCl_3$): 8.54–8.37 (16H, $AA'BB'_{Ar}$), 7.26–7.11 (16H, $AA'BB'_{benzo}$),), 4.51 (8H, m), 1.93 (8H, m), 1.62 (8H, m), 1.08 (12H, m); δ_C ($CDCl_3$): 167.1, 145.2, 137.9, 137.1, 133.9, 132.4, 130.8, 130.0, 125.7, 124.0, 116.8, 66.2, 31.2, 20.1, 14.2; MALDI, *m/z*: found 1278, calcd 1277 for $C_{80}H_{68}N_4O_8Zn$; UV–VIS, λ_{max} nm (DMF): 472 (1.0), 624 (0.07), 659 (0.14).

3.2.3. H_2 *meso*-(4-BuOOCC$_6$H$_4$)$_4$TBP. The green solid, obtained at the previous stage, was dissolved in 150 mL of CH_2Cl_2 and 25 mL of CF_3COOH was added. The mixture was stirred for 1 h. at rt. Formation of the porphyrin dication from the Zn complex could be conveniently monitored by UV–VIS spectroscopy. The obtained solution was washed with 200 mL of water, then with 200 mL of 1 M NaOH and again with 200 mL of water. The resulting mixture was dried over Na_2SO_4 and purified on a silica gel (100–200 mesh) column. The mixture, reduced in volume down to about 50 mL, was placed on the top of the column and first eluted with pure CH_2Cl_2. The first green fraction (~1%, R_f ≈0.4) was mass-spectroscopically identified as *meso*-diaryl tetrabenzoporphyrin, H_2 *meso*-(4-BuOOCC$_6$H$_4$)$_2$TBP (*m/z*: calcd 860, found 864). This fraction also contained a small amount of Pd *meso*-(4-BuOOCC$_6$H$_4$)$_4$TBP (**3**) (*m/z*: calcd 1318, found 1320). The following fraction (~12%, R_f ≈ 0.2), with slightly different shade of green color, was identified as *meso*-trisubstituted tetrabenzoporphyrin, H_2 *meso*-(4-BuOOCC$_6$H$_4$)$_3$TBP (*m/z*: calcd 1036, found 1040). The UV–VIS spectrum of the trisubstituted porphyrin is significantly different from the tetrasubstituted one, making it possible to follow the elution of this fraction spectroscopically. After elution was complete the eluent mixture was changed to CH_2Cl_2/THF=12:1, and the residual deep green fraction (~82%) was collected. The solvent was removed and an amorphous green solid (H_2 *meso*-(4-BuOOCC$_6$H$_4$)$_4$TBP) was dried in vacuum. Yield: 0.75 g, 1.3%. (The reported yield is based on phthalimide taken into the initial reaction). δ_H ($CDCl_3$): 8.59–8.48 (16H, $AA'BB'_{Ar}$), 7.28 (16H, bs_{benzo}), 4.57 (8H, t, *J*=6.6 Hz), 1.95 (8H, m), 1.69 (8H, m), 1.10 (12H, t, *J*=7.4 Hz); δ_C ($CDCl_3$): 166.7, 146.0, 134.7, 131.1, 130.1, 128.8, 127.6, 126.2, 124.2, 115.1, 65.3, 31.2, 19.3, 13.7; MALDI, *m/z*: found 1216, calcd 1214, for $C_{80}H_{70}N_4O_8$; UV–VIS, λ_{max} nm (DMF): 469 (1.0), 592 (0.07), 643 (0.16), 701 (0.03).

3.2.4. Pd *meso*-(4-BuOOCC$_6$H$_4$)$_4$TBP (3). H_2 *meso*-(4-BuOOCC$_6$H$_4$)$_4$TBP (0.2 g, 0.16 mmol) was dissolved in 100 mL of DMF and the solution was brought to boiling with continuous stirring. $PdCl_2$ (42 mg, 0.24 mmol) was added to the mixture in small portions during approximately 30 min period, until the UV–VIS spectra indicated that insertion of Pd into the porphyrin was complete. The mixture was cooled down, the solvent was removed by rotary evaporation and the remaining solid was dissolved in 50 mL of CH_2Cl_2. **3** was purified by chromatography on silica gel, using CH_2Cl_2/THF=12:1 mixture as the eluent. The solvent was removed and the product was dried in vacuum. Yield: 0.2 g, 95%. When synthesis of **3** was accomplished without intermediate separation and purification of Zn complex and free-base porphyrin, additional chromatography with toluene was required at this stage (see the main text). In this case the overall yield of **3**, based on phthalimide taken in the initial reaction was about 3%. δ_H ($CDCl_3$): 8.46–8.25 (16H, $AA'BB'_{Ar}$), 7.11–6.94 (16H, $AA'BB'_{benzo}$), 4.44 (8H, t, *J*=6.6 Hz), 1.82 (8H, m), 1.53 (8H, m), 0.97 (12H, t, *J*=7.36 Hz); δ_C ($CDCl_3$): 166.7, 145.9, 138.2, 137.6, 134.1, 132.9, 131.2, 130.3, 125.6, 123.8, 117.3, 65.4, 30.9, 19.4, 13.8; MALDI, *m/z*: found 1318, calcd 1318 for $C_{80}H_{68}N_4O_8Pd$; UV–VIS, λ_{max} nm (DMF): 443 (1.0), 584 (0.05), 632 (0.35).

3.2.5. Pd *meso*-(4-HOOCC$_6$H$_4$)$_4$TBP (4). Pd *meso*-(4-BuOOCC$_6$H$_4$)$_4$TBP (0.4 g, 0.3 mmol) was treated overnight with excess of NaOH (2 g, 50 mmol) in 30 mL of MeOH under stirring. 50 mL of H_2O was added to the resulting suspension, causing the green precipitate to dissolve. MeOH was removed under vacuum and **4** was precipitated from the solution upon addition of HCl. The precipitate was collected by centrifugation and dried in vacuum, giving **4** as an amorphous dark green powder. Yield: 0.32 g, 97%. δ_H

(DMSO-d_6): 8.47–8.32 (16H, AA′BB′$_{Ar}$), 7.27–6.92 (16H, AA′BB′$_{benzo}$); δ_C (DMSO-d_6): 167.0, 144.6, 137.2, 136.9, 133.6, 131.7, 130.1, 125.8, 123.1, 117.0; MALDI, *m/z*: found 1096, calcd 1094 for $C_{80}H_{68}N_4O_8Pd$; UV–VIS, λ_{max} nm (DMF): 442 (1.0), 582 (0.05), 629 (0.35).

3.2.6. PdTBP-Glu^{1}OEt (G1-Et). In a 200 mL flask, **4** (0.32 g, 0.29 mmol) was suspended in 100 mL of freshly distilled THF. Diethylglutamate hydrochloride Glu(OEt)$_2$ (0.7 g, 2.9 mmol), DCC (2.9 g, 1.0 mmol) and 0.5 mL of pyridine were added under continuous stirring and the mixture was allowed to react in the dark for 24 h at rt. The resulting deep green solution was filtered and the solvents were removed on a rotary evaporator, leaving a viscous green oil, which was re-dissolved again in 50 mL of CH_2Cl_2. The white crystalline precipitate was filtered off and the mixture was washed with three 100 mL portions of water. The organic phase was collected, dried over Na_2SO_4 and its volume was reduced to 25 mL by rotary evaporation. The chromatography on silica gel was carried out using CH_2Cl_2/THF=12:1 mixture. The first intense deep green band, coming after the solvent front, was collected. The solvent was removed and the resulting green solid (**G1-Et**) was dried in vacuum. Yield: 0.55 g, 96%. δ_H ($CDCl_3$): 8.42–8.37 (16H, AA′BB′$_{Ar}$), 7.61 (4H, d_{NH}, *J*= 7.0 Hz), 7.25–7.09 (16H, AA′BB′$_{benzo}$), 5.02 (4H, m), 4.37 (8H, m_{Et1}), 4.22 (8H, q_{Et2}, *J*=7.0 Hz), 2.67 (m, 8H), 2.50 (8H, m), 2.36 (8H, m), 1.42 (12H, t, *J*=7.0 Hz), 1.32 (12H, t, *J*=7.0 Hz); δ_C ($CDCl_3$): 173.0, 171.7, 166.9, 145.1, 138.3, 137.6, 134.3, 134.0, 128.0, 125.7, 123.8, 117.2, 52.8, 30.6, 27.2; MALDI, *m/z*: found 1835, calcd 1834 for $C_{100}H_{96}N_8O_{20}Pd$; UV–VIS, λ_{max} nm (DMF): 442 (1.0), 583 (0.05), 633 (0.35).

3.2.7. PdTBP-Glu^{1}OH (G1). G1-Et. (0.45 g, 0.24 mmol), 5 mL of THF, 5 mL of MeOH and LiOH (1 g, 40 mmol) were stirred together at rt for 0.5 h, and a green suspension formed. H_2O (50 mL) were added to the mixture, causing the precipitate to dissolve. MeOH and THF were removed on a rotary evaporator, and the resulting dark green solution was filtered. The solution was neutralized by addition of HCl and filtered again through a 0.45 μm nitrocellulose filter to remove microscopic solid impurities. **G1** was precipitated by addition of HCl. The precipitate was collected by centrifugation, washed with distilled water and dried in vacuum, giving **G1** as a dark green powder. Yield: 0.38 g, 97%. δ_H (DMSO-d_6): 9.21 (4H, d_{NH}, *J*= 11.7 Hz), 8.51–8.40 (16H, AA′BB′$_{Ar}$), 7.36–7.06 (16H, AA′BB′$_{benzo}$), 4.60 (4H, m), 2.50 (8H, m), 2.20 (8H, m); δ_C (dmso-d_6): 173.8, 173.3, 166.2, 143.4, 137.5, 137.0, 134.6, 133.4, 128.5, 125.9, 123.3, 117.2, 52.3, 30.5, 26.1; MALDI, *m/z*: found 1610, calcd 1610 for $C_{84}H_{64}N_8O_{20}Pd$; UV–VIS, λ_{max} nm (DMF): 441 (1.0), 582 (0.05), 633 (0.35).

3.2.8. PdTBP-Glu^{1}PEG350 (G1-PEG350). G1 (20 mg, 0.012 mmol), BtOH (84 mg, 0.62 mmol), DCC (0.128 g, 0.62 mmol) and 2 drops of *sym*-collidine were stirred in 3 mL of PEG350 (polyethylene glycol monomethyl ether, Av. MW 350) for 3 days at rt 5 mL of water and one drop of HCl were added to the mixture and it was left in the fridge in the dark overnight. The resulting mixture was neutralized and the solution was filtered through a paper filter (Whatman, Grade 5) and then through a 0.45 μm nitrocellulose filter to remove all solid impurities. **G1-PEG350** was purified by GPC on a Biorad S-X1 column and then on a Sephadex G50 column. The collected solution was lyophilized, leaving dark green viscous material, well soluble in organic solvents (CH_2Cl_2, ether, MeOH) and in water. Yield: 50 mg, 90%. δ_H ($CDCl_3$): 8.51–8.21 (32H, bm AA′BB′$_{Ar}$ and AA′BB′$_{benzo}$), 7.79 (4H, m), 5.01 (4H, m), 4.43 (8H, m), 4.29 (8H, m), 3.80–3.75 (16H$_{PEG350}$, m), 3.72–3.55 (~230H$_{PEG350}$, m), 3.51–3.30 (24H$_{PEG350}$, m), 2.70 (8H, m), 2.46 (4H, m), 2.32 (8H, m); δ_C ($CDCl_3$): 173.3, 171.9, 166.8, 145.0, 138.3, 137.6, 134.3, 128.0, 125.7, 123.8, 117.2, 71.9, 70.6(broad), 68.9(broad), 64.5(broad), 58.9, 52.8, 30.6, 27.3; MALDI, *m/z*: found ~4208 (broad peak), calcd 4266, assuming MW of PEG 350; UV–VIS, λ_{max} nm (DMF): 442 (1.0), 582 (0.05), 633 (0.35).

3.2.9. PdTBP-Glu^{2}OEt (G2-Et). In a 100 mL flask, **4** (0.15 g, 0.093 mmol) was suspended in 50 mL of freshly distilled THF. Diglutamic dendron tetraethylester (0.48 g, 0.93 mmol), BtOH (0.13 g, 0.93 mmol), DCC (0.19 g, 0.93 mmol) and 2 drops of *sym*-collidine were added to the mixture under continuous stirring and mixture was allowed to react in the dark for 10 days at rt. The dark green solution was filtered and THF was removed on a rotary evaporator. The resulting viscous material was redissolved in 50 mL of $CHCl_2$ and washed with water in a separatory funnel. The organic phase was collected, dried over Na_2SO_4, filtered and its volume was reduced to about 20 mL by rotary evaporation. The mixture was chromatographed on silica gel and eluted with CH_2Cl_2/THF=5:1 mixture. **G2-Et** was additionally purified by GPC on a Biorad S-X1 column. The intense deep green band was collected, the solvent was removed and the resulting dark green solid was dried in vacuum. Yield: 0.18 g, 63%. δ_H ($CDCl_3$): 8.45–7.22 (m AA′BB′$_{Ar}$ and NH, 28H), 7.25–7.05 (m AA′BB′$_{benzo}$, 16H), 4.90–4.75 (m, 12H), 4.40–4.20 (m, 32H), 2.80–2.25 (m, 48H), 1.8–1.5 (m, 48H); δ_C (DMSO-d_6): 173.7(broad), 171.8(broad), 166.3, 143.6, 137.7, 137.2, 134.9, 128.7, 126.2, 123.6, 117.3, 64.5, 62.1, 51.4, 34.1, 26.1, 23.4; MALDI, *m/z*: found 3093 (M^+), 2779, 2464, 2150; calcd 3092 for $C_{156}H_{184}N_{16}O_{44}Pd$; UV–VIS, λ_{max} nm (DMF): 443 (1.0), 582 (0.05), 633 (0.35).

3.2.10. PdTBP-Glu^{2}OH (G2). G2 was synthesized from **G2-Et** (0.15 g, 0.048 mmol) in the same way as **G1** was synthesized from **G1-Et** (synthesis 3.2.7). Yield: 0.12 g, 97%. δ_H (DMSO-d_6): 9.4–8.9 (8H, m_{NH}), 8.53–8.26 (20H, AA′BB′$_{Ar}$+m_{NH}), 7.37–7.07 (16H, AA′BB′$_{benzo}$), 4.63 (4H, m), 4.28 (8H, m), 2.60–2.25 (12H, m), 2.25–1.70 (12H, m); δ_C (DMSO-d_6): 173.3(b), 171.9(b), 166.3, 143.6, 137.7, 137.2, 134.9, 133.6, 128.8, 126.1, 123.5, 117.4, 53.6–51.5(b), 32.2–30.3(b), 27.8–26.6(b); MALDI, *m/z*: found 2644 (M^+), 2513, 2379, 2247, 2118, 1986, 1856; calcd 2642 for $C_{124}H_{120}N_{16}O_{44}Pd$; UV–VIS, λ_{max} nm (DMF): 443 (1.0), 583 (0.05), 634 (0.34).

3.2.11. PdTBP-Glu^{2}PEG350 (G2-PEG350). G2 (30 mg, 1.13×10^{-2} mmol), BtOH (62 mg, 0.45 mmol), DCC (93 mg, 0.45 mmol) and 2 drops of *sym*-collidine were stirred in 5 mL of PEG350. The work-up of the mixture followed synthesis Section 3.2.8 described above. **G2-PEG350** was isolated as dark green viscous material. Yield: 78 mg, 88%. δ_H ($CDCl_3$): 8.52–7.33 (44H, bm AA′BB′$_{Ar}$,

$AA'BB'_{benzo}$ and NH), 4.67 (32H, m), 4.32 (4H, m), 4.21 (8H, m), 3.58 ($326H_{PEG350}$, m), 3.35 ($\sim 508H_{PEG350}$, m), 2.60–2.14 (8H, m); δ_C ($CDCl_3$): 172.5, 171.3, 145.0, 138.3, 137.7, 134.2, 130.5, 128.2, 125.7, 123.8, 117.3, 71.9, 70.6, 69.1, 64.5, 63.8, 58.9, 53.2, 30.3, 26.7; MALDI, *m/z*: found 7800 (broad peak), calcd 7954 assuming MW of PEG 350; UV–VIS, λ_{max} nm (DMF): 443 (1.0), 583 (0.04), 633 (0.34).

3.2.12. PdTBP-Glu^{3}OEt (G3-Et). G3-Et was synthesized in the same fashion as **G1-Et** (synthesis from Section 3.2.6), from **G2** (0.2 g, 7.57×10^{-2} mmol), $Glu(OEt)_2$ (0.87 g, 3.63 mmol), BtOH (0.49 g, 3.63 mmol), DCC (0.75 g, 3.63 mmol) and 2 drops of *sym*-collidine in 20 mL of DMF. Chromatographic purification: silica gel, CH_2Cl_2/pyridine=10:1 mixture; GPC S-X1, THF. **G3-Et** was isolated as a dark green solid. Yield: 178 mg, 42%. δ_H ($CDCl_3$): 8.5–7.3 (m $AA'BB'_{Ar}$ and NH, 44H), 7.25–7.00 (m $AA'BB'_{benzo}$, 16H), 4.76–4.12 (m, 92H), 2.59–1.83 (m, 112H), 1.31 (m, 96H); δ_C ($CDCl_3$): 173.2, 170.1, 163.3, 145.7, 138.1, 137.7, 134.8, 128.1, 126.3, 124.0, 116.8, 65.1, 62.1, 51.3, 34.1, 26.1; MALDI, *m/z*: found 5606 (M^+), 5293, 4978; calcd 5606 for $C_{268}H_{360}N_{32}O_{92}Pd$; UV–VIS, λ_{max} nm (DMF): 443 (1.0), 584 (0.04), 634 (0.36).

3.2.13. PdTBP-Glu^{3}OH (G3). G3 was synthesized from **G3-Et** (0.15 g, 2.7×10^{-2} mmol) using the same conditions as in the case of **G2** (synthesis from Section 3.2.10). **G3** was isolated as a dark green amorphous solid. Yield: 120 mg, 96%. δ_H (dmso-d_6): 9.35–8.85 (4H, m_{NH}), 8.49–8.37 (16H, $AA'BB'_{Ar}$), 8.28–8.13 (24H, m_{NH}), 7.31–7.06 (16H, $AA'BB'_{benzo}$), 4.8–4.1 (28H, m), 4.28 (8H, m), 2.60–1.6 (112H, m); δ_C (DMSO-d_6): 173.6, 171.9, 166.5, 143.5, 137.6, 137.2, 134.5, 133.5, 128.7, 126.0, 123.5, 117.5, 51.3, 31.8, 30.2, 26.5; UV–VIS, λ_{max} nm (DMF): 443 (1.0), 584 (0.04), 634 (0.35).

3.2.14. PdTBP-Glu^{4}OEt (G4-Et). G4-Et was synthesized in the same fashion as **G3-Et** (synthesis from Section 3.2.12), using **G3** (60 mg, 1.27×10^{-2} mmol), $Glu(OEt)_2$ (0.29 g, 1.22 mmol), BtOH (0.16 g, 1.22 mmol), DCC (0.25 g, 1.22 mmol) and 2 drops of *sym*-collidine in 20 mL of DMF. **G4-Et** was isolated as a dark green solid. Chromatographic purification: GPC S-X1, THF, two times. Yield: 47 mg, 35%. δ_H ($CDCl_3$): 8.4–7.3 (m $AA'BB'_{Ar}$ and NH, 76H), 7.2–7.06 (m $AA'BB'_{benzo}$, 16H), 4.8–4.6 (m, 60H), 4.20 (m, 128H), 2.56–1.82 (m, 240H), 1.25 (m, 192H); δ_C ($CDCl_3$) (all signals are significantly broadened): 173.0, 170.1, 163.5, 145.6, 138.2, 137.6, 134.7, 128.7, 126.1, 123.8, 116.6, 64.5, 62.0, 51.2, 34.6, 32.0, 26.7; MALDI, *m/z*: found 10634 (M^+), 10318, 10005, 9691, 9376, 9061, 8746, 8432, 8119, 7806, 7491; calcd 10630 for $C_{492}H_{712}N_{64}O_{188}Pd$; UV–VIS, λ_{max} nm (DMF): 444 (1.0), 584 (0.04), 635 (0.34).

3.2.15. PdTBP-Glu^{4}OH (G4). G4 was synthesized from **G4-Et** (40 mg, 3.7×10^{-3} mmol) using the same conditions as in the case of dendrimer **G2** (synthesis from Section 3.2.13). It was isolated as an extremely hygroscopic green powder Yield: 31 mg, 95%. δ_H (D_2O): 8.58 (bm, 16H), 7.30–7.00 (m, $AA'BB'_{benzo}$), 4.80–4.20 (m, 60H), 2.85–1.80 (m, 240H); δ_C (D_2O): 182.01, 181.8, 179.6, 176.0, 143.8, 138.1, 137.9, 135.1, 134.6, 127.9, 128.0, 122.7, 113.3, 56.7, 55.2, 54.1, 36.0, 34.2, 33.6, 32.6, 29.2, 28.7, 28.1, 25.9, 25.1. In the ^{13}C NMR spectrum of **G4** the peaks in the glutamate region (60–20 ppm) consist of multiple resonances and appear as broadened. UV–VIS, λ_{max} nm (H_2O, pH 8.0): 442 (1.0), 581 (0.03), 631 (0.33).

Acknowledgements

Supported by the grants NS-31465 and CA-74062 from the National Institutes of Health. Authors thank Professor David F. Wilson for many invaluable discussions.

References

1. For selected reviews, see: (a) Smith, D. K.; Diederich, F. *Chem. Eur. J.* **1998**, *4*, 1353–1361. (b) Fischer, M.; Vögtle, F. *Angew. Chem. Int. Ed.* **1999**, *38*, 885–905. (c) Vögtle, F.; Gestermann, S.; Hesse, R.; Schwierz, H.; Windisch, B. *Prog. Polym. Sci.* **2000**, *25*, 987–1041. (d) Dykes, G. M. *J. Chem. Tech. Biotech.* **2001**, *76*, 903–918. (e) Grayson, S. K.; Fréchet, J. M. J. *Chem. Rev.* **2001**, *101*, 3819–3867.
2. (a) Krause, W.; Hackmann-Schlichter, N.; Maier, F.; Muller, R. Dendrimers in diagnostics. In *Dendrimers II. Architecture, Nanostructure and Supramolecular Chemistry*. *Topics in Current Chemistry*; Vögtle, F., Ed.; Springer: New York, 2000; Vol. 210, pp 261–308. (b) Stiriba, S. E.; Frey, H.; Haag, R. *Angew. Chem. Int. Ed.* **2002**, *41*, 1329–1334.
3. (a) Hecht, S.; Fréchet, J. M. J. *Angew. Chem. Int. Ed.* **2001**, *40*, 74–91. (b) Gorman, C. B.; Smith, J. C. *Acc. Chem. Res.* **2001**, *34*, 60–71.
4. For a review, see: Demas, J. N.; DeGraff, B. A.; Coleman, P. B. *Anal. Chem.* **1999**, *71*, 793A–800A.
5. (a) Vanerkooi, J. M.; Maniara, G.; Green, T. J.; Wilson, D. F. *J. Biol. Chem.* **1987**, *262*, 5476–5482. (b) Wilson, D. F.; Rumsey, W. L.; Green, T. J.; Vanderkooi, J. M. *J. Biol. Chem.* **1988**, *263*, 2712–2718. (c) Rumsey, W. L.; Vanderkooi, J. M.; Wilson, D. F. *Science* **1988**, *241*, 1649.
6. (a) Pawlowski, M.; Wilson, D. F. *Adv. Exp. Med. Biol.* **1992**, *316*, 179–185. (b) Wilson, D. F.; Cerniglia, G. *Cancer Res.* **1992**, *52*, 3988–3992. (c) Vinogradov, S. A.; Lo, L.-W.; Jenkins, W. T.; Evans, S. M.; Koch, C.; Wilson, D. F. *Biophys. J.* **1996**, *70*, 1609–1617. (d) Shonat, R. D.; Wachman, E. S.; Niu, W. H.; Koretsky, A. P.; Farkas, D. L. *Biophys. J.* **1997**, *73*, 1223–1231. (e) Howlett, R. A.; Hogan, M. C. *J. Appl. Physiol.* **2001**, *91*, 632–636. (f) Bonanno, J. A.; Stickel, T.; Nguyen, T.; Biehl, T.; Carter, D.; Benjamin, W. J.; Soni, P. S. *Invest. Ophthalmol. Visual Sci.* **2002**, *43*, 371–376. (g) Smith, L. M.; Golub, A. S.; Pittman, R. N. *Microcirculation* **2002**, *9*, 389–395.
7. Molar solubility of O_2 at 298 K and 1 atm is 1.278 mM in H_2O. In *Solubility of Gases in Liquids*; Fogg, P. G. T., Gerrard, W., Eds.; Wiley: New York, 2001.
8. (a) Issberner, J.; Vögtle, F.; De Cola, L.; Balzani, V. *Chem. Eur. J.* **1997**, *3*, 706–712. (b) Vögtle, F.; Plevoets, M.; Nieger, M.; Azzellini, G. C.; Credi, A.; De Cola, L.; De Marchis, V.; Venturi, M.; Balzani, V. *J. Am. Chem. Soc.* **1999**, *121*, 6290–6298.
9. (a) Jin, R. H.; Aida, T.; Inoue, S. *J. Chem. Soc., Chem. Commun.* **1993**, 1260–1262. (b) Sadamoto, R.; Nobuyuki, T.; Aida, T. *J. Am. Chem. Soc.* **1996**, *118*, 3978–3979. (c) Pollak,

K. W.; Leon, J. W.; Fréchet, J. M. J.; Maskus, M.; Abruna, H. D. *Chem. Mater.* **1998**, *10*, 30–38. (d) Matos, M. S.; Hofkens, J.; Verheijen, W.; De Schryver, F. C.; Hecht, S.; Pollak, K. W.; Fréchet, J. M. J.; Forier, B.; Dehaen, W. *Macromolecules* **2000**, *33*, 2967–2973. (e) Riley, J. M.; Alkan, S.; Chen, A. D.; Shapiro, M.; Khan, W. A.; Murphy, W. R.; Hanson, J. E. *Macromolecules* **2001**, *34*, 1797–1809. (f) Cardona, C. M.; Wilkes, T.; Ong, W.; Kaifer, A. E.; McCarley, T. D.; Pandey, S.; Baker, G. A.; Kane, M. N.; Baker, S. N.; Bright, F. V. *J. Phys. Chem. B* **2002**, *106*, 8649–8656.

10. (a) Diederich, F.; Felber, B. *Proc. Natl Acad. Sci. USA* **2002**, *99*, 4778–4781, and references therein. (b) Van Doorslaer, S.; Zingg, A.; Schweiger, A.; Diederich, F. *ChemPhysChem* **2002**, *3*, 659–667. (c) Weyermann, P.; Diederich, F.; Gisselbrecht, J. P.; Boudon, C.; Gross, M. *Helv. Chim. Acta* **2002**, *85*, 571–598. (d) Weyermann, P.; Diederich, F. *Helv. Chim. Acta* **2002**, *85*, 599–617. (e) Zingg, A.; Felber, B.; Gramlich, V.; Fu, L.; Collman, J. P.; Diederich, F. *Helv. Chim. Acta* **2002**, *85*, 333–351. (f) Uyemura, M.; Aida, T. *J. Am. Chem. Soc.* **2002**, *124*, 11392–11403.
11. (a) Capitosti, G. J.; Cramer, S. J.; Rajesh, C. S.; Modarelli, D. A. *Org. Lett.* **2001**, *3*, 1645–1648. (b) Rajesh, C. S.; Capitosti, G. J.; Cramer, S. J.; Modarelli, D. A. *J. Phys. Chem. B* **2001**, *105*, 10175–10188.
12. (a) Bhyrappa, P.; Young, J. K.; Moore, J. S.; Suslick, K. S. *J. Am. Chem. Soc.* **1996**, *118*, 5708–5711. (b) Bhyrappa, P.; Vaijayanthimala, G.; Suslick, K. S. *J. Am. Chem. Soc.* **1999**, *121*, 262–263. (c) Kimura, M.; Shiba, T.; Yamazaki, M.; Hanabusa, K.; Shirai, H.; Kobayashi, N. *J. Am. Chem. Soc.* **2001**, *123*, 5636–5642. (d) Zhang, J. L.; Zhou, H. B.; Huang, J. S.; Che, C. M. *Chem. Eur. J.* **2002**, *8*, 1554–1562.
13. (a) Jiang, D. L.; Aida, T. *J. Am. Chem. Soc.* **1998**, *120*, 10895–10901. (b) Choi, M. S.; Aida, T.; Yamazaki, T.; Yamazaki, I. *Chem. Eur. J.* **2002**, *8*, 2668–2678. (c) Onitsuka, K.; Kitajima, H.; Fujimoto, M.; Iuchi, A.; Takei, F.; Takahashi, S. *Chem. Commun.* **2002**, 2576–2577.
14. (a) Vinogradov, S. A.; Wilson, D. F. *Adv. Exp. Med. Biol.* **1997**, *428*, 657–662. (b) Vinogradov, S. A.; Lo, L. W.; Wilson, D. F. *Chem. Eur. J.* **1999**, *5*, 1338–1347.
15. (a) Rozhkov, V. V.; Wilson, D. F.; Vinogradov, S. A. *Polym. Mater. Sci. Eng.* **2001**, 601–603. (b) Rozhkov, V.; Wilson, D.; Vinogradov, S. *Macromolecules* **2002**, *35*, 1991–1993.
16. Adler, A. D.; Longo, F. R.; Shergalis, W. D. *J. Am. Chem. Soc.* **1964**, *86*, 3145–3149.
17. Lindsey, J. S.; Schreiman, I. C.; Hsu, H. C.; Kearney, P. C.; Marguerettaz, A. M. *J. Org. Chem.* **1987**, *52*, 827–836.
18. Eastwood, D.; Gouterman, M. J. *Mol. Spectr.* **1970**, *35*, 359–375.
19. (a) Papkovsky, D. B.; Ponomarev, G. V.; Trettnak, W.; Oleary, P. *Anal. Chem.* **1995**, *67*, 4112–4117. (b) Papkovsky, D. B.; Ponomarev, G. V.; Wolfbeis, O. S. *Spectrochim. Acta A-Mol. Biomol. Spectr.* **1996**, *52*, 1629–1638.
20. (a) Vinogradov, S. A.; Wilson, D. F. *J. Chem. Soc., Perkin Trans. 2* **1994**, 103–111. (b) Vinogradov, S. A.; Wilson, D. F. *Adv. Exp. Med. Biol.* **1997**, *411*, 597–603.
21. (a) Kimura, M.; Nakada, K.; Yamaguchi, Y.; Hanabusa, K.; Shirai, H.; Kobayashi, N. *Chem. Commun.* **1997**, 1215–1216. (b) Brewis, M.; Clarkson, G. J.; Goddard, V.; Helliwell, M.; Holder, A. M.; McKeown, N. B. *Angew. Chem. Int. Ed.* **1998**, *37*, 1092–1094. (c) Kimura, M.; Sugihara, Y.; Muto, T.; Hanabusa, K.; Shirai, H.; Kobayashi, N. *Chem. Eur. J.* **1999**, *5*, 3495–3500. (d) Brewis, M.; Helliwell, M.; McKeown, N. B.; Reynolds, S.; Shawcross, A. *Tetrahedron Lett.* **2001**, *42*, 813–816.
22. For review see: Lash, T. D. In *The Porphyrin Handbook. Syntheses of novel porphyrinoid chromophores*; Kadish, K. M., Smith, K. M., Guilard, R., Eds.; Academic: New York, 2000; Vol. 2, pp 125–199.
23. (a) Kopranenkov, V. N.; Dashkevich, S. N.; Luk'yanets, E. A. *J. Gen. Chem. (Russ)* **1981**, *51*, 2165–2168. (b) Remy, D. E. *Tetrahedron Lett.* **1983**, *24*, 1452–1454.
24. (a) Vicente, M. G. H.; Tome, A. C.; Walter, A.; Cavaleiro, J. A. S. *Tetrahedron Lett.* **1997**, *38*, 3639–3642. (b) Ito, S.; Murashima, T.; Uno, H.; Ono, N. *Chem. Commun.* **1998**, 1661–1662. (c) Ito, S.; Uno, H.; Murashima, T.; Ono, N. *Tetrahedron Lett.* **2001**, *42*, 45–47. (d) Finikova, O.; Cheprakov, A.; Beletskaya, I.; Vinogradov, S. *Chem. Commun.* **2001**, 261–262.
25. Ichimura, K.; Sakuragi, M.; Morii, H.; Yatsuike, M.; Fukui, M.; Ohno, O. *Inorg. Chim. Acta* **1991**, *182*, 83–86.
26. Vinogradov, S. A.; Wilson, D. F. *Tetrahedron Lett.* **1998**, *39*, 8935–8938.
27. (a) Dandliker, P. J.; Diederich, F.; Gisselbrecht, J. P.; Louati, A.; Gross, M. *Angew. Chem. Int. Ed. Engl.* **1996**, *34*, 2725–2728. (b) Dandliker, P. J.; Diederich, F.; Zingg, A.; Gisselbrecht, J. P.; Gross, M.; Louati, A.; Sanford, E. *Helv. Chim. Acta* **1997**, *80*, 1773–1801.
28. (a) Liu, M.; Kono, K.; Fréchet, J. M. J. *J. Polym. Sci. A Polym. Chem.* **1999**, *37*, 3492–3503. (b) Liu, M.; Kono, K.; Fréchet, J. M. J. *J. Controlled Release* **2000**, *65*, 121–131.
29. Twyman, L.; Beezer, A. E.; Mitchell, J. C. *Tetrahedron Lett.* **1994**, *35*, 4423–4424.
30. For examples see: (a) Maiti, N. C.; Mazumdar, S.; Periasamy, N. *J. Phys. Chem. B* **1998**, *102*, 1528–1538. (b) Khairutdinov, R. F.; Serpone, N. *J. Phys. Chem. B* **1999**, 761–769, and references therein.
31. (a) Cheng, R. J.; Chen, Y. R.; Wang, S. L.; Cheng, C. Y. *Polyhedron* **1993**, *12*, 1353–1360. (b) Finikova, O. S.; Cheprakov, A. V.; Carroll, P. J.; Dalosto, S.; Vinogradov, S. A. *Inorg. Chem.* **2002**, *41*, 6944–6946.
32. Callis, J. B.; Knowles, J. M.; Gouterman, M. *J. Phys. Chem.* **1973**, *77*, 154–156.
33. To our knowledge, glucose/glucose oxidase/catalase system is the most effective O_2 scavenger for aqueous solutions.
34. Tomoyose, Y.; Jiang, D. L.; Jin, R. H.; Aida, T.; Yamashita, T.; Horie, K.; Yashima, E.; Okamoto, Y. *Macromolecules* **1996**, *29*, 5236–5238.
35. The quenching constants in the PdTCPP-series have been measured using a different experimental setup[14].
36. (a) Phillips, D. *Analyst* **1994**, *119*, 543–550. (b) Borissevitch, I. E.; Tominaga, T. T.; Imasato, H.; Tabak, M. J. *Luminescence* **1996**, *69*, 65–76.
37. Dunphy, I.; Vinogradov, S. A.; Wilson, D. F. *Analyt. Biochem.* **2002**, *310*, 191–198.
38. Vinogradov, S. A.; Fernandez-Seara, M. A.; Dugan, B. W.; Wilson, D. F. *Rev. Sci. Instrum.* **2001**, *72*, 3396–3406.
39. Koch, C. J. Canadian Patent 1992, June 30, 1304449.
40. Seybold, P. G.; Gouterman, M. *J. Mol. Spectrosc.* **1969**, *31*, 1.
41. Quimby, D. J.; Longo, F. R. *J. Am. Chem. Soc.* **1975**, *97*, 5111–5117.